

## Burst kinetics of single NMDA receptor currents in cell-attached patches from rat brain cortical neurons in culture

Nancy W. Kleckner and Barry S. Pallotta\*

*Department of Pharmacology, School of Medicine, University of North Carolina, Chapel Hill, NC 27599-7365, USA*

1. The patch-clamp technique was used to record single-channel currents from cell-attached patches on rat brain cortical neurons in culture. The composition of the open and shut intervals during bursts of openings was studied in *N*-methyl-D-aspartate (NMDA) receptors exposed to 1  $\mu\text{M}$  NMDA and 10  $\mu\text{M}$  glycine at a membrane potential of  $-70$  mV.
2. Open interval histograms were constructed for openings at each position (first, second, third, etc.) during all bursts. Distributions from openings two to five were fitted with similar (two or three) exponential components. The first opening from all bursts tended to be of shorter duration than the other openings.
3. Bursts were sorted according to the number of openings they contained and duration histograms were obtained for the openings at each position (one to five) during bursts of up to five openings. For bursts containing two or more openings, the distribution of open durations obtained at a given position were similar to each other regardless of the number of openings in the burst.
4. In bursts of two or more openings (up to five), duration histograms from the openings at each position in the burst were fitted with two or three exponential components that were similar for each opening. Bursts consisting of a single opening had a different distribution, having a relatively larger component of short duration.
5. Shut intervals during bursts were described by two exponential components with average time constants (and relative areas) (means  $\pm$  s.e.m.) of  $0.06 \pm 0.01$  ms ( $0.59 \pm 0.02$ ) and  $0.64 \pm 0.02$  ms ( $0.41 \pm 0.02$ ). Their distribution was independent of the numbers of openings in the bursts, their position within the burst, and the types of openings (long or short duration) contained within the burst.
6. These results suggest that each opening in bursts of two or more openings is kinetically similar to every other opening regardless of burst length. Analogously, each shut period during a burst was similar to every other. A kinetic model with three open and four closed intraburst states is shown to be consistent with these results for bursts of two or more openings.

*N*-Methyl-D-aspartate (NMDA) receptors are an important subclass of glutamate receptor that respond to the binding of particular extracellular excitatory amino acids by allowing a transient flux of cations across the cell membrane (see reviews by Beal, 1992; Hollmann & Heinemann, 1994; McBain & Mayer, 1994). This current of  $\text{Na}^+$ ,  $\text{K}^+$  and  $\text{Ca}^{2+}$  underlies both electrical and metabolic ( $\text{Ca}^{2+}$ ) signalling, and is controlled by a complex gating mechanism. Single-channel studies have revealed the existence of at least three open and five closed kinetic states (Jahr & Stevens, 1990;

Howe, Cull-Candy & Colquhoun, 1991; Gibb & Colquhoun, 1992) and several conductance levels (Cull-Candy & Usowicz, 1987; Jahr & Stevens, 1987; Howe *et al.* 1991; Gibb & Colquhoun, 1992). As observed for other ligand-gated channels (Colquhoun & Sakmann, 1981; Magleby & Pallotta, 1983*a,b*; Macdonald, Rogers & Twyman, 1989), some channel openings occur in rapid succession (bursts), while others occur singly in apparent isolation from other openings. In the case of NMDA receptors, the bursts themselves can be grouped into clusters that seem to arise

\* To whom correspondence should be addressed.

from a single channel activation, that is, after a single agonist binding event (Gibb & Colquhoun, 1992). The lengths of these clusters can account for the prolonged channel activity that is observed after relatively brief exposures to agonists (Lester, Clements, Westbrook & Jahr, 1990; Gibb & Colquhoun, 1991; Edmonds & Colquhoun, 1992). During bursts and clusters of openings, any of the kinetically distinguishable open states can occur, although bursts with more than one opening have a relatively larger proportion of intermediate- and long-duration openings compared with single-opening bursts (Gibb & Colquhoun, 1992). Although the general composition of the open and shut intervals during bursts is thus known, the kinetic characteristics of these events have yet to be examined with respect to the position of the event within the burst, or to the length of the burst. This information might identify unique features of the gating mechanism that must be part of any proposed model for channel activation (Colquhoun & Hawkes, 1982).

In this paper we present an analysis of the duration of channel openings and closings that occurred within bursts of openings. NMDA (1  $\mu\text{M}$ ) and saturating glycine (10  $\mu\text{M}$ ) were used to evoke openings from NMDA receptors in membrane patches attached to rat brain cortical neurons in culture. Duration histograms were constructed for openings at each position (first, second, third, etc.) during a burst, and also for the shut intervals during a burst. We found that the distributions obtained for the openings at each position in bursts of two or more openings were indistinguishable from one another, and did not depend on the number of openings in the bursts. A similar result was found for the shut intervals during bursts. When compared with each other, distributions of shut intervals from each position during a burst were nearly the same. These distributions were also independent of the length of the burst, and also of the types of opening (short or long duration) contained within the burst. These results are summarized by a novel kinetic model for channel bursting behaviour that contains three open and four closed intra-burst states.

## METHODS

### Neuronal culture

The procedure for obtaining neurons was similar to that described in Hoch & Dingledine (1986). Briefly, E19 fetuses were removed from pregnant Sprague-Dawley rats under ether anaesthesia. Brain cortical tissue was removed under a dissecting microscope, minced and incubated at 37 °C for 30 min in  $\text{Ca}^{2+}$ - and  $\text{Mg}^{2+}$ -free Hank's balanced salt solution (HBSS) containing 0.3% protease and 0.3% collagenase (Sigma). The cells were then dispersed by gentle trituration in 2 ml fortified modified Eagle's medium (MEM) with 0.01 mg ml<sup>-1</sup> DNase and diluted in MEM. Neurons were then plated at a density of 100–500 cells cm<sup>-2</sup> onto plastic coverslips coated with poly-D-lysine and maintained in a humid 95% air–5% CO<sub>2</sub> atmosphere at 37 °C. Subsequent feedings

(every 3–5 days) consisted of serum-free medium. Cells were used for electrical recordings after 8–10 days in culture.

### Patch-clamp techniques

Cell-attached patches allowed long, stable recordings of channel activity from channels that are relatively undisturbed compared with an excised patch. In addition, these patches contained, on average, fewer channels than outside-out patches, thus simplifying kinetic analyses. The patch-clamp technique for recording currents from individual ion channels has been well described (Sakmann & Neher, 1983). Electrodes were made from N51A borosilicate glass (Drummond Scientific, Broomall, PA, USA) and were coated with Sylgard (Dow Corning, Midland, MI, USA) at the tip to reduce noise and stray capacitances. To control the membrane potential, cells were first depolarized by perfusion with a solution containing 110–130 mM KCl. The potential across the patch was then set to –70 mV. NMDA and glycine were present in the recording electrode.

### Solutions and agonist application

All drugs and salts were dissolved in water from a Nanopure system (Barnstead/Thermolyne, Dubuque, IA, USA). The external bath solution contained (mM): 150 NaCl, 2.5 KCl, 2 CaCl<sub>2</sub> and 10 Hepes; pH 7.4, 290–300 mosmol l<sup>-1</sup>. The depolarizing solution contained (mM): 110–130 KCl, 22.5–42.5 NaCl, 0.5 CaCl<sub>2</sub> and 10 Hepes. This solution was applied either through a U tube (Krishtal & Pidoplichko, 1980) lowered to within 100  $\mu\text{m}$  of the cell, or via the bath perfusion. Pipette solution was similar to the external bath solution except that NMDA (1  $\mu\text{M}$ ) and glycine (10  $\mu\text{M}$ ) were added. Rapid application of agonists was unnecessary because currents were recorded only during the steady state. In addition, CaCl<sub>2</sub> was reduced to 0.5 mM to increase the size of the unitary currents (Ascher & Nowak, 1988; Gibb & Colquhoun, 1992). Throughout each experiment cells were continuously perfused with fresh bath solution at a rate of approximately 1–2 ml min<sup>-1</sup>.

To minimize any contribution from voltage-dependent  $\text{Mg}^{2+}$  block at negative potentials (Nowak, Bregestovski, Ascher, Herbet & Prochiantz, 1984), ultrapure KCl, NaCl (Fluka, Ronkonkoma, NY, USA) and CaCl<sub>2</sub> (Alfa Johnson Matthey, Ward Hill, MA, USA) were used in all solutions. In the depolarizing solution, the estimated contaminant  $\text{Mg}^{2+}$  (0.84  $\mu\text{M}$ ) was much less than the concentration giving half-maximal inhibition ( $K_i$ ) for  $\text{Mg}^{2+}$  block (32.5  $\mu\text{M}$ ; Ascher & Nowak, 1988) expected at the one membrane potential (–70 mV) used in this study. Apparent channel closures due to block would thus be negligible. It is also possible that external  $\text{Ca}^{2+}$ , entering the cells upon depolarization, might affect channel kinetics (see Gibb & Colquhoun, 1992; McBain & Mayer, 1994). However, we do not think that significant effects occurred because the distributions we obtained for both open and (especially) shut intervals were similar to those found when divalent ions are reduced by EDTA in both cell-attached and excised outside-out configurations (Gibb & Colquhoun, 1992).

### Data acquisition and analysis

**Interval detection.** Single-channel currents were stored on magnetic tape (Racal 4DS FM recorder) and later digitized for off-line analysis. Because channel open and closed times were of interest, single-channel currents were reduced to a sequence of open and closed times by an algorithm that measured these durations with respect to a 50% threshold. To set the threshold, amplitude distributions were constructed from the individual

Table 1. Summary of data sets

Experiment no.	No. of intervals	$nP_o$	Total time (min)	Burst $t_c$ (ms)	Open $t_c$ (ms)	No. of bursts
1	49799	0.030	36	1.28	0.19	15 186
2	6107	0.003	22	2.27	0.15	1811
3	8436	0.010	12	1.10	0.19	2734
4	4860	0.004	25	1.86	0.14	1501
5	17 316	0.002	14	1.06	0.17	5589
6	18 023	0.001	27	1.37	0.19	6040
7	11 702	0.006	31	1.25	0.21	4368

$nP_o$  is the steady-state probability of opening;  $t_c$  is the critical time.

sample points so that baseline and open-channel current levels (and their standard deviations) could be measured. The threshold was then adjusted to 50% of the difference between the two and analog filtering was adjusted until the standard deviation of the baseline noise was approximately 5-fold smaller than the threshold (Colquhoun & Sigworth, 1983). Once the filter was set, currents were sampled at intervals of one-third to one-fifth of the system dead time (Magleby, 1992). Open and shut times measured by this technique were multiples of the sample interval (typically 12.5  $\mu$ s), and were corrected for binning aliasing errors during histogram construction (Magleby, 1992) by the method of Korn & Horn (1988).

**Fitting distributions.** Interval histograms were constructed as in Sigworth & Sine (1987), and fitted to sums of exponentials by an algorithm that maximized the likelihood of observing the binned data. The fitting process was begun with the minimal number of exponential components that gave a reasonable fit by eye. Additional components were added if a log-likelihood ratio test (Horn, 1987; McManus & Magleby, 1988) demonstrated significant improvement ( $P < 0.05$ ) in the fit. Likelihood calculations were restricted to (binned) intervals with durations greater than 1.5–2 times the system dead time (Magleby, 1992), and only those intervals included in the fitting process are shown in the figures. In some cases, shorter duration intervals were included in the fit to ensure that a substantial component of the distribution was not ignored (see also Howe *et al.* 1991). No other corrections for missed events were applied. Errors and 95% confidence limits for the areas and time constants for each fitted component were determined from 2-unit likelihood intervals (Colquhoun & Sigworth, 1983).

**Comparing distributions.** To determine if two sets of intervals were drawn from the same (or different) distribution, interval distributions (100 linear bins) were compared with each other by calculating a  $\chi^2$  statistic from the two distributions in question (Press, Teukolsky, Vetterling & Flannery, 1992). Two distributions were considered significantly different from each other if the  $\chi^2$  probability was  $< 0.05$ . The sensitivity of this method was tested with simulations of simple kinetic schemes that predicted similar three-component distributions of open intervals to those reported here (Fig. 1D). When simulated distributions contained 1000 intervals, the  $\chi^2$  test revealed a significant difference between distributions if the relative areas for each component differed by approximately 50% from the corresponding components in the other distribution. Distributions containing approximately 150 intervals were found to be significantly different only if the relative areas differed by a factor of two.

These results were in agreement with simple visual comparisons: only those distributions that appeared different to the eye were, in fact, statistically dissimilar.

**Definition of bursts.** Bursts were defined as groups of open and shut intervals that were preceded and followed by shut intervals that exceeded a particular critical time ( $t_c$ ). All shut intervals less than the critical time were assumed to reside within bursts. Two methods were used to calculate  $t_c$ . The *numbers* method (Magleby & Pallotta, 1983a) calculates  $t_c$  by finding the shut time at which equal numbers of shut intervals would be incorrectly classified as intraburst *vs.* interburst. The *proportions* method (Colquhoun & Sakmann, 1985) derives  $t_c$  as the shut time at which equal proportions of intra- and interburst intervals were misclassified. Both methods gave similar results. Both methods also required an assignment of one or more components of the shut interval distribution as intra- or interburst gaps. As in Howe *et al.* (1991) and Gibb & Colquhoun (1992), we assumed that the two shortest duration components of the shut interval distribution were within bursts.

**Model predictions.** The various interval distributions obtained by experiment were qualitatively compared with the predictions of several different kinetic schemes. Theoretical distributions for each proposed model were evaluated numerically according to Colquhoun & Hawkes (1981, 1982), or by computer simulation.

**Multiple channels in a patch.** Most patches contained an unknown number of channels. Useful kinetic information could still be obtained because it is likely that each burst of openings contains only openings from one particular channel (Colquhoun & Sakmann, 1981). If the channels are similar to each other and there are few overlapping events, then the kinetic information pertaining to bursting behaviour will be valid (Colquhoun & Hawkes, 1990). This is not true of the longest closed times in the experimental record, however, since these intervals will vary (inversely) with the number of channels in the patch. As a result, we have not attempted to describe the longer closed times with a kinetic model. These arguments were verified for our particular conditions by performing kinetic analyses upon data from a computer-simulated multi-channel patch. Given the generally low steady-state channel activity that we observed (Table 1), simulations based upon models of the types described later showed that, as expected, only the longest duration shut times were affected by the presence of more than one channel. This occurred because in our experiments the longest shut times were usually much longer than any of the others.

**Channel subconductances.** NMDA receptors open to at least five different conductance levels, with most opening in our experiments to the main level of approximately 50 pS (0.5 mM extracellular  $\text{Ca}^{2+}$ ) (Ascher & Nowak, 1988; Gibb & Colquhoun, 1992). However, most patches contained few subconductance states, and their occurrence would not be expected to influence our conclusions. Occasionally a patch contained numerous channel openings to subconductance levels; such recordings were not subjected to kinetic analysis.

Unless otherwise stated, all values given are means  $\pm$  S.E.M.

## RESULTS

Seven cell-attached patches exposed to 1  $\mu\text{M}$  NMDA and 10  $\mu\text{M}$  glycine ( $-70$  mV) were selected for detailed analysis based upon the large numbers of intervals that were obtained from each, and the stability of channel activity during the recording period (Table 1). Under these conditions the steady-state probability of opening ( $nP_o$ ) in these patches was low, ranging from 0.001 to 0.030 (see Fig. 1A). Given these low levels of activity, bursts of channel openings most probably arose from the activation of one channel at a time even though each patch probably contained more than one active channel (Colquhoun & Sakmann, 1981). Our analysis was therefore restricted to the kinetics of opening and closing during bursts. In one experiment (no. 5), open and shut intervals measured during occasional periods of high open probability (Jahr & Stevens, 1987; Howe *et al.* 1991) were omitted from the analysis.

### Open and shut interval distributions

Unconditional distributions of shut intervals were used to calculate the burst critical gap for each data set. The distribution obtained from experiment no. 5 is shown in Fig. 1B, in which the channel closed times were best described by the sum of five exponential components (see legend). For all experiments, the average shut distribution time constants (and relative areas) were  $0.10 \pm 0.01$  ms ( $0.20 \pm 0.01$ ),  $0.74 \pm 0.11$  ms ( $0.16 \pm 0.01$ ),  $13.50 \pm 3.10$  ms ( $0.16 \pm 0.02$ ),  $125.4 \pm 27.0$  ms ( $0.22 \pm 0.03$ ) and  $779 \pm 277$  ms ( $0.26 \pm 0.03$ ). The variability between patches is illustrated in Fig. 1C, in which a symbol (different for each patch) is plotted at the intersection of each fitted time constant and its relative area. The groupings of the symbols show that the distribution time constants were well separated from each other in most patches, although there is some overlap between the fourth and fifth components. This is probably a consequence of multiple-channel activity in the patches (see Methods), which would cause the longest shut times to appear shorter in proportion to the number of active channels. To divide channel openings into bursts, we assumed that intervals from the two shortest components occurred within bursts, while clusters were assumed to contain the shortest three (Howe *et al.* 1991; Gibb & Colquhoun, 1992). For the

distribution shown in Fig. 1B, the critical time for defining bursts was 1.06 ms.

For comparison with the open interval durations we found during particular types of bursts, unconditional distributions of open intervals obtained for each data set were fitted with sums of exponential components. Figure 1D shows the distribution for the same patch as in B. In six patches the average time constants (and relative areas) for the three-component fits were  $0.06 \pm 0.01$  ms ( $0.32 \pm 0.05$ ),  $1.65 \pm 0.18$  ms ( $0.37 \pm 0.08$ ) and  $3.33 \pm 0.35$  ms ( $0.31 \pm 0.05$ ) (filled symbols, Fig. 1E). One data set (no. 2), however, was better fitted with two exponential components (open circles in Fig. 1E). Similar distributions for both shut and open intervals have been previously reported for NMDA receptors activated by 10–30  $\mu\text{M}$  NMDA in outside-out patches from rat cerebellar granule cells (Howe *et al.* 1991) or by 20–100 nM glutamate in cell-attached or inside-out patches from adult rat hippocampus (Gibb & Colquhoun, 1992).

### Openings during bursts

Gibb & Colquhoun (1992) showed that single-opening bursts and bursts of more than one opening contain short-, intermediate- or long-duration openings. Compared with single-opening bursts, multiple-opening bursts tend to have longer duration openings. We have extended this analysis by examining the composition of opening durations that occurred at each position within all bursts, and also during bursts of specific numbers of openings (i.e. burst length).

Figure 2 shows the lifetime distribution of the first (B), second (C), third (D) or fourth (E) opening from all 15186 bursts in experiment no. 1 (distributions obtained from bursts with different lengths and from openings at specific positions within the bursts are described below). In each case the open times were described by three exponentials, indicating that short-, intermediate- or long-duration openings could occur at any position within a burst. However, the distribution of first openings (B) is clearly different from the distributions of the other openings. Similar results were found in all patches. Except for the first opening, the open interval histograms from each position were fitted with similar exponential components, although some patches were better fitted with two components instead of three. For the four patches in which distributions of second openings were fitted with three components, the average time constants (and relative areas) were  $0.08 \pm 0.01$  ms ( $0.18 \pm 0.02$ ),  $2.28 \pm 0.08$  ms ( $0.60 \pm 0.06$ ) and  $4.53 \pm 0.28$  ms ( $0.22 \pm 0.06$ ). The third openings from all bursts in two experiments were fitted with three components of  $0.08 \pm 0.01$  ms ( $0.17 \pm 0.01$ ),  $2.40 \pm 0.09$  ms ( $0.60 \pm 0.05$ ) and  $4.72 \pm 0.35$  ms ( $0.22 \pm 0.05$ ). Whether the distributions were fitted with two or three components did not affect the overall result; that is, except

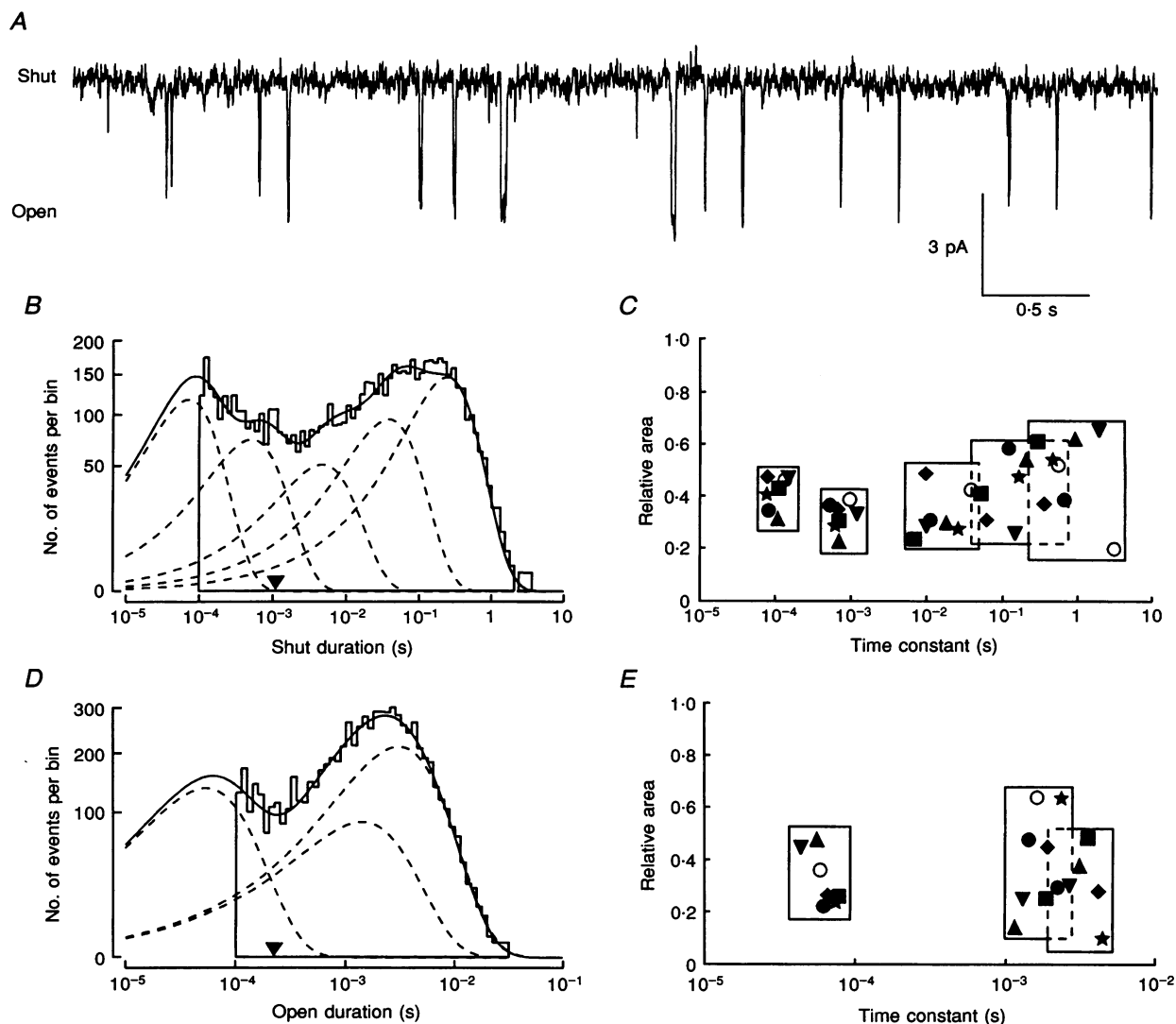


**Figure 1. Distributions of open and shut intervals**

*A*, continuous 5 s recording of single-channel currents obtained from a cell-attached patch at  $-70$  mV with  $1 \mu\text{M}$  NMDA and  $10 \mu\text{M}$  glycine in the pipette (experiment no. 5). The trace was low-pass filtered at 100 Hz for display purposes to illustrate the average level of activity observed in most patches ( $nP_o = 0.002$  in this patch). At higher resolution (Fig. 2*A*), the (downward) openings are better resolved and reach the same maximum current. *B*, histogram of 8624 shut intervals was fitted with a sum of five exponential components with time constants (and relative areas) of 0.08 ms (0.27), 0.61 ms (0.15), 5.51 ms (0.10), 46.65 ms (0.19) and 311.81 ms (0.29). The calculated 1.06 ms critical gap ( $t_c$ ) that was used to delineate 5589 bursts of openings is indicated by the arrowhead. Currents were digitized at 80 kHz and low-pass filtered at 2.5 kHz (experiment no. 5). In this and all subsequent histograms, the individual fitted components are drawn as dashed lines, while the sum of the components is drawn as a continuous line. *C*, graph of relative areas and time constants obtained from all five-component fits to the distributions of shut intervals. Each symbol represents a time constant and corresponding relative area for each component. The boxes enclose the values for each of the five components. Each data set is represented by a different symbol: no. 1,  $\blacklozenge$ ; no. 5,  $\blacksquare$ ; no. 7,  $\blacktriangle$ ; no. 4,  $\blacktriangledown$ ; no. 6,  $\blackstar$ ; no. 2,  $\circ$ ; no. 3,  $\bullet$ . *D*, histogram of 8630 open intervals was fitted with a sum of three exponential components with time constants (and relative areas) of 0.06 ms (0.31), 1.57 ms (0.20) and 3.38 ms (0.49). The arrowhead indicates the calculated 0.17 ms critical gap that was used in this experiment to sort individual openings as either long or short duration (experiment no. 5). *E*, summary of relative areas and time constants obtained from all three-component fits to the distributions of open intervals. In one experiment (no. 2), two exponential components gave a better fit than three components. Symbols as in *C*.

for the first opening (*B*), the time constants and relative proportions of each type of opening did not depend on position within the burst.

### Openings during bursts of specified length

The above results show that the lifetimes and proportions of short-, intermediate- and long-duration openings did not depend on when the opening occurred in the burst.

However, those distributions included openings from bursts of various lengths so that any differences between bursts of different lengths were obscured. Therefore, we examined the distributions of openings from bursts with specific numbers of openings. Figure 3*A* shows the distribution of the first opening in bursts of one opening (i.e. single-opening bursts). As with the results of Gibb & Colquhoun (1992), these openings were either short-, intermediate- or

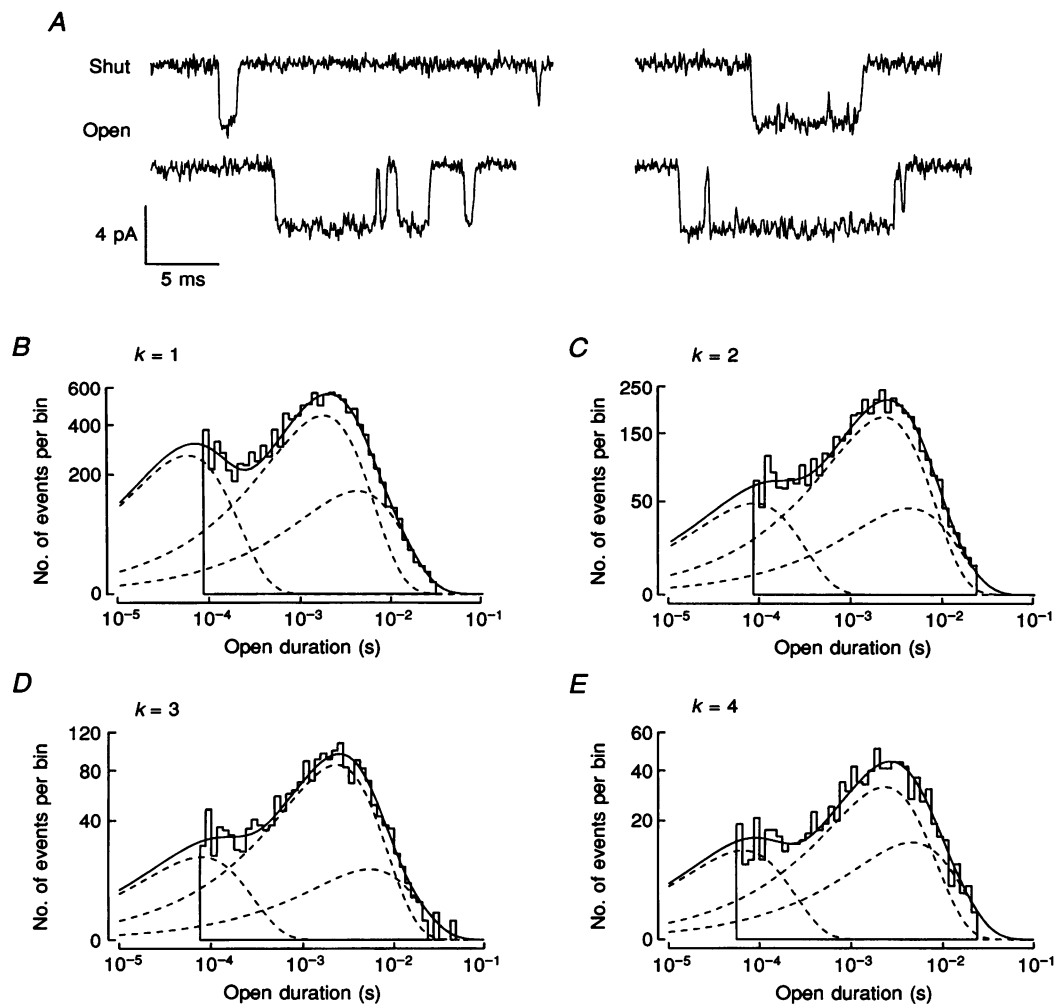


**Figure 2.** Distributions of the first (*B*), second (*C*), third (*D*) or fourth (*E*) opening during all bursts

*A*, sample current traces illustrate bursts of one or more openings. The left traces show two single-opening bursts (top) and a burst with three openings followed by a single opening (bottom). The right traces show a burst with two openings (top) and three openings (bottom). Currents were filtered at 2.5 kHz (experiment no. 5). *B*, distribution of the first ( $k = 1$ ) openings from all bursts. The histogram contains 15 080 intervals and was fitted with three components with time constants (and relative areas) of 0.06 ms (0.31), 1.94 ms (0.52) and 4.56 ms (0.17). The histograms in this figure were obtained from experiment no. 1. Currents were low-pass filtered at 3.2 kHz and sampled at 80 kHz. In this and other figures,  $k$  is the opening number. *C*, distribution of the second ( $k = 2$ ) openings from all bursts. The histogram contains 5030 intervals and was fitted with time constants (and relative areas) of 0.10 ms (0.18), 2.51 ms (0.66) and 4.77 ms (0.16). *D*, distribution of the third ( $k = 3$ ) openings from all bursts. The histogram contains 2164 intervals and was fitted with time constants (and relative areas) of 0.09 ms (0.16), 2.69 ms (0.72) and 6.25 ms (0.12). *E*, distribution of the fourth ( $k = 4$ ) openings from all bursts. A total of 1040 intervals were fitted with time constants (and relative areas) of 0.08 ms (0.20), 2.69 ms (0.57) and 5.33 ms (0.23). Note the similarities in the fits for openings two to four.

long duration. Compared with the distribution of all openings (Fig. 1D), single-opening bursts had a slightly larger contribution from short-duration openings (see legend). For all patches, the average fitted constants to the single-opening durations (and relative areas) were  $0.05 \pm 0.01$  ms ( $0.47 \pm 0.03$ ),  $1.26 \pm 0.21$  ms ( $0.25 \pm 0.06$ ) and  $2.73 \pm 0.25$  ms ( $0.28 \pm 0.05$ ). Openings from bursts with more than one opening were markedly different. Compared with the distribution of all openings, or to the single-opening bursts (Fig. 3A), lengthier bursts contained a larger proportion of long-duration openings. However, this proportion did not depend on the burst length itself. Figure 3 shows the distribution of the *second* opening (for example) from bursts of two (B), three (C) or four (D) openings. In each case, the distributions were similar in appearance and fitted components (see legend). Similar results were found in all patches: that is, the distributions of second openings in all patches during bursts of up to four openings were independent of the number of openings in the burst. This conclusion was supported by the similarities in the appearance and fitted constants for

each distribution. Taken together, these results suggest that each open interval during a burst is similarly distributed regardless of position within the burst or the length of the burst. Distributions from the other openings during bursts also supported this conclusion, and are described below.

### Burst symmetry

Most models for ion channel gating are constructed from discrete kinetic states (open and closed) that interconvert with rate constants that are independent of previous channel activity. Direct support for these assumptions comes from adjacent-states analysis (Blatz & Magleby, 1989), which shows that the mean lifetime of the NMDA receptor open states does not depend on the mean lifetime of the adjacent-occurring closed periods (Gibb & Colquhoun, 1992). Another property of such Markov-type gating follows from considerations of microscopic reversibility: at steady state, bursts of openings should be symmetrical in that the lifetime distribution of the first opening should be the same as that for the last opening, that of the second opening should be similar to the second-to-last opening, and so on (Colquhoun & Hawkes, 1982). The results shown

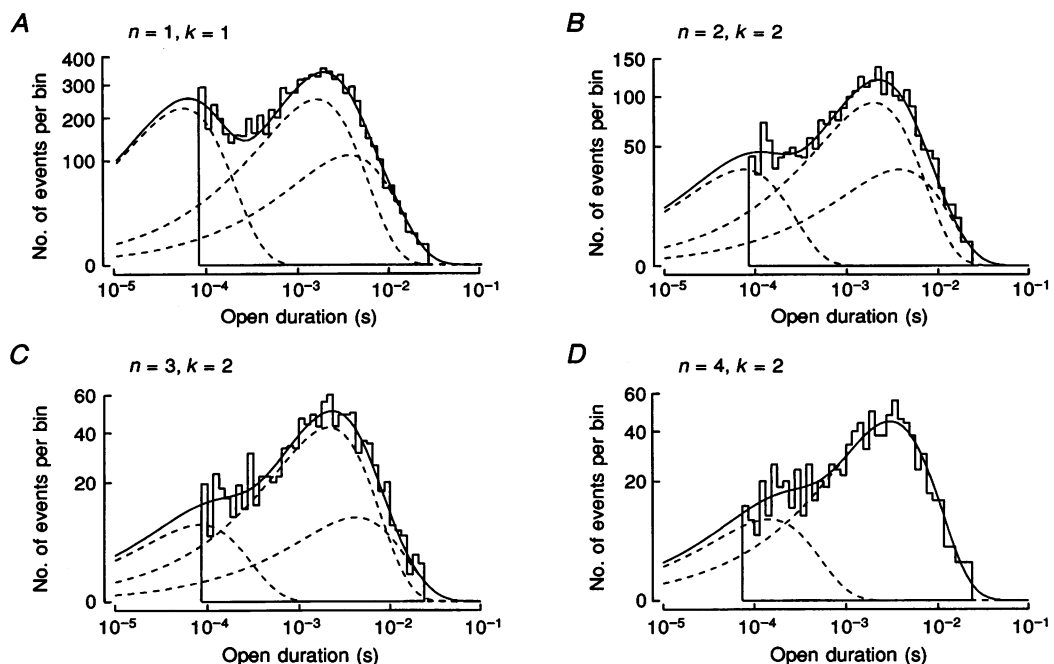


**Figure 3.** Distributions of openings from bursts of one (A), two (B), three (C) or four (D) openings

A, histogram of 10 042 single-opening bursts ( $n = 1$ ) was fitted with three exponential components with time constants (and relative areas) of 0.06 ms (0.38), 1.75 ms (0.43) and 3.99 ms (0.19). Currents were sampled at 80 kHz and low-pass filtered at 3.2 kHz (experiment no. 1). B, distribution of the second opening ( $k = 2$ ) from bursts that contained only two openings ( $n = 2$ ). The histogram contains 2862 intervals fitted with time constants (and relative areas) of 0.09 ms (0.21), 2.29 ms (0.59) and 4.35 ms (0.20). C, distribution of the second opening ( $k = 2$ ) from bursts of only three openings ( $n = 3$ ). In total, 1124 intervals were fitted with three time constants (and relative areas) of 0.11 ms (0.13), 2.35 ms (0.60) and 4.34 ms (0.27). D, distribution of the second opening ( $k = 2$ ) from bursts of only four openings ( $n = 4$ ). The relatively small number of intervals (513) were better fitted with two time constants (and relative areas) of 0.17 ms (0.17) and 3.46 ms (0.83) than with three components (see McManus & Magleby, 1988).

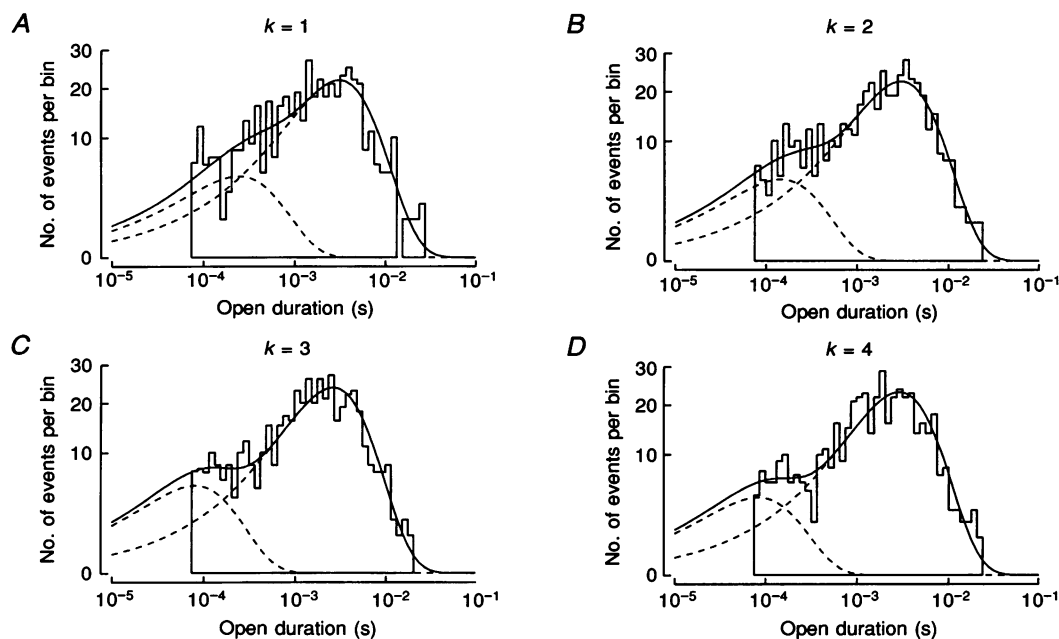
in Fig. 2 (openings at each position within various length bursts) and Fig. 3 (the second opening from bursts of known lengths) already imply that this might be the case. Therefore, we directly tested this prediction for bursts of up to six openings (see below) and found that bursts were indeed symmetrical. Consistent with the above results, the distribution of each opening (from multiple-opening bursts) was indistinguishable from the distribution of any other opening.

Figure 4 shows the distributions of open times for each opening from four-opening bursts. Each histogram appears similar to the others, and all were best fitted with similar exponential components (see legend). In this case, each distribution was fitted with only two components because there were insufficient numbers of intervals to define a third component in each histogram.  $\chi^2$  comparisons (see Methods) between the distributions of the first opening (*A*) and the distributions of each of the other openings (*B–D*) found no significant differences between them. Similar results were found when first openings were compared with each of the others in bursts of two openings ( $n = 7$  patches), three openings ( $n = 7$ ), four openings ( $n = 7$ ), five openings ( $n = 1$ ) and six openings ( $n = 1$ ). These results suggest a straightforward conclusion: in multiple-opening bursts, each

opening had the same kinetic characteristics as every other opening.

#### Shut intervals during bursts of specified length

In light of the above findings for burst openings, distributions of shut intervals during bursts were examined for similar types of relationships. As described in the Discussion, such information might be used to specify a unique model or class of models that describe the gating of NMDA receptors. Figure 5 shows the distribution of all shut times during bursts of two (*A*), three (*B*), or four (*C*) openings. The distributions are truncated at the right because shut times longer than the critical time (1.28 ms in this experiment) were assumed to be gaps between bursts and were excluded from these distributions. As is apparent in the figure, the histograms appear alike and were fitted with similar time constants and relative areas (see legend). Similar results were found in all seven patches. For bursts of two openings the fitted time constants (and relative areas) were  $0.08 \pm 0.01$  ms ( $0.55 \pm 0.02$ ) and  $0.71 \pm 0.05$  ms ( $0.45 \pm 0.02$ ); for three-opening bursts,  $0.06 \pm 0.01$  ms ( $0.59 \pm 0.03$ ) and  $0.59 \pm 0.03$  ms ( $0.41 \pm 0.03$ ); and for four-opening bursts,  $0.06 \pm 0.01$  ms ( $0.64 \pm 0.03$ ) and  $0.61 \pm 0.01$  ms ( $0.36 \pm 0.03$ ).  $\chi^2$  comparisons (three patches) between the first shut interval and each of the others in the



**Figure 4.** Distributions of the first (*A*), second (*B*), third (*C*) or fourth (*D*) opening from bursts of four openings

*A*, the first openings from bursts containing four openings were fitted with the sum of two exponential components with time constants (and relative areas) of 0.28 ms (0.17) and 3.57 ms (0.83). The histograms in this figure were fitted with two components because the relatively small numbers of intervals in each (514) did not consistently support a third component (experiment no. 1). *B*, histogram of second openings was fitted with time constants and (relative areas) of 0.17 ms (0.17) and 3.46 ms (0.83). *C*, histogram of the third opening from each burst was fitted with time constants and (relative areas) of 0.09 ms (0.18) and 3.07 ms (0.82). *D*, fourth (and last) openings were fitted with time constants (and relative areas) of 0.10 ms (0.15) and 3.37 ms (0.85).



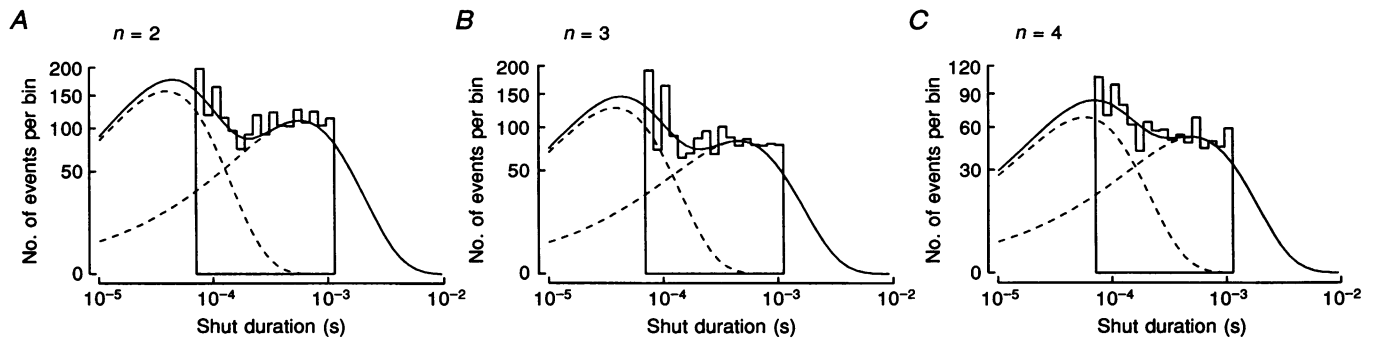


**Figure 5. Distribution of shut intervals during bursts that contained two (A), three (B) or four (C) openings**

A, 2848 shut intervals from bursts of only two openings ( $n = 2$ ) were fitted with the sum of two exponential components with time constants (and relative areas) of 0.05 ms (0.59) and 0.69 ms (0.41). Note the absence of intervals longer than the critical gap of 1.28 ms (experiment no. 1). B, 2223 shut intervals from bursts of only three openings ( $n = 3$ ) were fitted with two time constants (and relative areas) of 0.05 ms (0.61) and 0.56 ms (0.39). C, 1530 shut intervals from bursts of only four openings ( $n = 4$ ) were fitted with time constants (and relative areas) of 0.07 ms (0.57) and 0.62 ms (0.43).

burst also indicated that the distributions from each shut interval were similar. These results are analogous to those described above for the open times – the relative occurrence of each type of shut interval during a burst was independent of the length of the burst.

**Symmetry of burst shut intervals**

As shown above, openings during bursts are symmetrical in that the distribution of the first opening was similar to that of the last, while the distribution of the second opening was similar to that of the second-to-last opening, etc. This was also the case for the shut intervals during bursts.

Figure 6 shows distributions of burst shut intervals obtained from bursts containing only four openings (and three shut

intervals). The distributions obtained from the first (Fig. 6A), second (B) and third (C) shut intervals do not appear different from each other. Fits to these distributions (see legend) were sufficiently alike to suggest that the underlying distributions for each shut interval during a burst were similar to each other. Similar results were found in all patches and  $\chi^2$  probabilities calculated from the differences between the distributions of first shut intervals and each of the others (in bursts of up to five openings) revealed no significant differences between any of the distributions. From the three experiments that yielded sufficient numbers of four-opening bursts for reliable fits to the shut intervals, the distribution of the first shut interval had fitted time constants (and relative areas) of  $0.06 \pm 0.01$  ms ( $0.61 \pm 0.01$ ) and  $0.57 \pm 0.07$  ms ( $0.39 \pm 0.01$ ); second

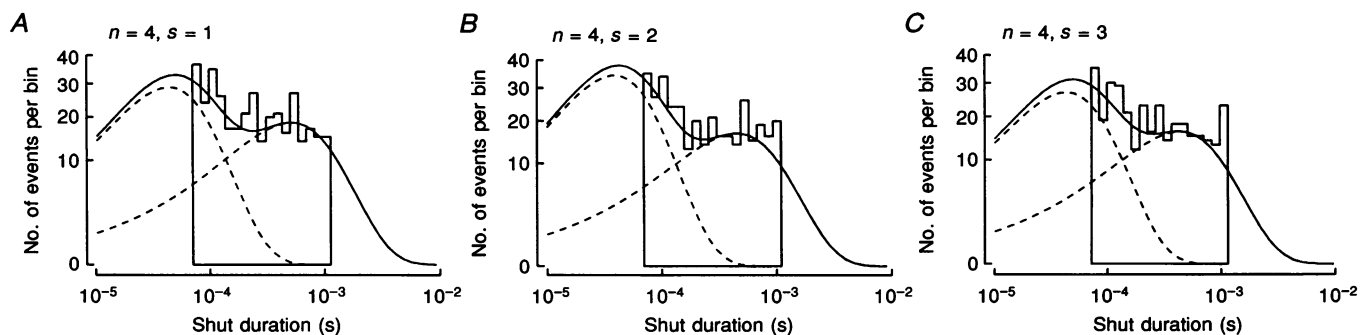


**Figure 6. Distributions of shut intervals from bursts that contained only four openings**

A, the distribution of first shut intervals ( $s = 1$ ) in bursts of four openings ( $n = 4$ ) were fitted with the sum of two exponential components with time constants (and relative areas) of 0.05 ms (0.61) and 0.63 ms (0.39). The distributions in this figure each contained 507 intervals (experiment no. 1). B, the second ( $s = 2$ ) shut intervals from the same set of four-opening bursts were fitted with time constants (and relative areas) of 0.05 ms (0.67) and 0.56 ms (0.33). C, the third (and last;  $s = 3$ ) shut intervals from the same set of four-opening bursts were fitted with time constants (and relative areas) of 0.05 ms (0.63) and 0.52 ms (0.37).

shut intervals had components of  $0.05 \pm 0.01$  ms ( $0.57 \pm 0.05$ ) and  $0.44 \pm 0.06$  ms ( $0.43 \pm 0.05$ ); and third shut intervals had components of  $0.06 \pm 0.01$  ms ( $0.59 \pm 0.04$ ) and  $0.40 \pm 0.05$  ms ( $0.41 \pm 0.04$ ). These results are analogous to those described above for openings: each shut interval during a burst seems to be much like every other. For bursts of two to four openings, the average time constants (and relative areas) for all shut intervals were  $0.06 \pm 0.01$  ms ( $0.59 \pm 0.02$ ) and  $0.64 \pm 0.02$  ms ( $0.41 \pm 0.02$ ).

#### Shut intervals in bursts without short-duration openings

The above results were obtained from bursts that were sorted according to the numbers of openings they contained, but not according to the types of openings. It is possible, for example, that the distribution of shut times during bursts composed of only short-duration openings might differ from that during bursts of only intermediate- or long-duration openings.

To test this possibility, distributions of shut times were constructed from bursts of different lengths, but the analysis was further restricted to those bursts containing only intermediate- and long-duration openings. These bursts were identified by sorting the open intervals during bursts into two classes: intervals less than a critical open time were deemed *short* duration, with the remaining intermediate- and long-duration openings classified as *long* duration (see arrowhead in Fig. 1D). Histograms of shut intervals from bursts that contained no short-duration openings are shown in Fig. 7 for burst lengths of two (A), three (B) and four (C) openings. A comparison of the histograms themselves and the fitting constants (see legend)

shows that these distributions are not only similar to each other, but also to those obtained from all bursts of various lengths (Fig. 5) and from bursts of a specific number of openings (Fig. 6). Similar results were obtained from all patches. For bursts containing two openings, the fitted time constants (and relative areas) for the shut interval distributions were  $0.06 \pm 0.01$  ms ( $0.57 \pm 0.02$ ) and  $0.64 \pm 0.05$  ms ( $0.43 \pm 0.02$ ); for bursts of three openings,  $0.09 \pm 0.02$  ms ( $0.57 \pm 0.03$ ) and  $0.62 \pm 0.04$  ms ( $0.44 \pm 0.03$ ); and for bursts of four openings,  $0.07 \pm 0.01$  ms ( $0.60 \pm 0.02$ ) and  $0.64 \pm 0.02$  ms ( $0.40 \pm 0.02$ ). These results suggest that the relative proportions of the two types of shut intervals within bursts did not depend on which type(s) of openings the bursts contained.

## DISCUSSION

The object of this study was to determine the kinetic characteristics of the openings and closings that occur during bursts of openings evoked by NMDA. Starting with the unconditional distribution of shut times, openings were grouped into bursts by assuming that the two shortest shut interval components resided within bursts, while the three longer components represented the interburst kinetic states. Burst structure was then analysed with respect to the durations of the openings and closings during bursts, and to the position at which these events occurred within the burst. We found that each opening of a multiple-opening burst was kinetically similar to every other: each opening had a 17% chance to be short duration (0.08 ms), a 60% chance to be intermediate (2.4 ms), and a 23% chance to be long duration (4.7 ms). Shut times during bursts were also similar to each other: 60% of the shut intervals were short

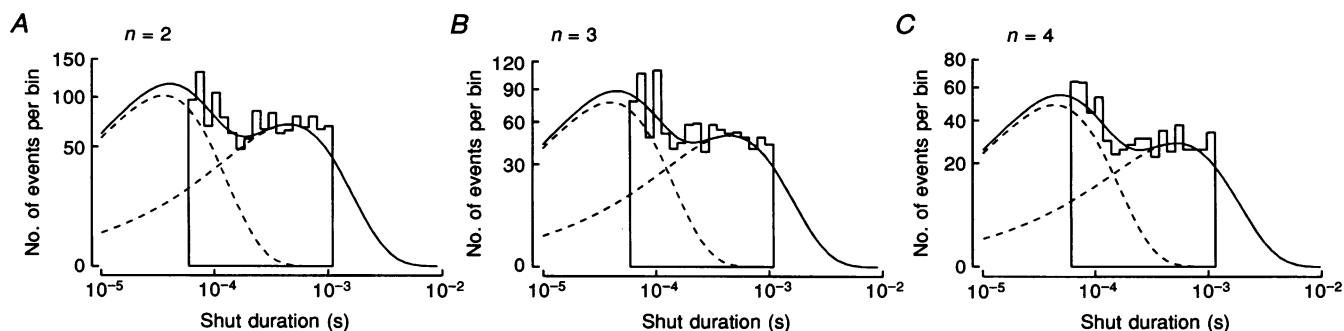


**Figure 7.** Distribution of shut intervals during bursts of two (A), three (B) or four (C) long-duration openings

Openings briefer than the critical gap of 0.19 ms (experiment no. 1) were classified as short duration, and all other openings were classified as long duration (the latter therefore contained openings from both the intermediate- and long-duration open-duration components). Bursts that contained only long-duration openings were then found, and distributions of shut intervals were obtained from these bursts of various lengths. A, the distribution of 1938 shut intervals from bursts that contained only two long-duration openings were fitted with time constants (and relative areas) of 0.04 ms (0.59) and 0.57 ms (0.41). B, shut intervals from bursts that contained three long openings were fitted with time constants (and relative areas) of 0.05 ms (0.61) and 0.57 ms (0.31). The histogram contains 1397 intervals. C, 839 shut intervals from bursts of four long openings were fitted with time constants (and relative areas) of 0.05 ms (0.63) and 0.63 ms (0.37).

duration (0.06 ms), with the remainder long duration (0.64 ms). These results are summarized in Fig. 8A, in which the open times during a diagrammatic burst of unspecified length each have the same average duration (2.5 ms), as do each of the shut times during the bursts (0.3 ms). For comparison with the results from multiple-opening bursts, Fig. 8B summarizes the distribution of open intervals obtained from single-opening bursts.

Our conclusions are based upon comparisons between the distributions of open and shut intervals at each position within a burst. The bases for comparison were the visual appearance of the distributions, the time constants and relative areas for the fitted exponential components, and  $\chi^2$  probabilities. Of the many distributions compared with each other, there was only one instance in which all three criteria did not agree. With no evidence to the contrary, we therefore concluded that no significant differences existed between distributions obtained from any one opening (or closing) *versus* any other. With respect to this conclusion, however, not all the comparisons carried equal weight. For example, we found that the first and last openings of bursts had the same distribution, as did the second and second-to-last openings, etc. Since this result is expected from thermodynamic considerations (Colquhoun & Hawkes,

1982), the similarity between the first and last openings does not alone support the conclusion that each and every opening of a burst has the same distribution. The stronger evidence for this conclusion comes from comparisons between openings that are not thermodynamically constrained, such as the first and second openings in bursts with at least three openings. Since the latter comparisons did not reveal any differences in any of the open (or shut) interval distributions, our conclusions seem to be justified.

Our results from NMDA receptors are similar to those obtained from nicotinic acetylcholine receptors at the frog muscle endplate (Colquhoun & Sakmann, 1985). With acetylcholine, suberyldicholine or decamethonium as agonist, the mean lengths of the openings and gaps during bursts showed no dependence on burst length or position within the burst. With respect to GABA<sub>A</sub> receptors, however, our results differ in some respects. Twyman, Rogers & Macdonald (1990) found that, in bursts of a given length, the distributions for each of the openings were similar to each other, as we have shown here for NMDA receptors. However, in GABA<sub>A</sub> receptor bursts the proportion of openings that are long duration increased with burst length. This was not the case for NMDA receptors, as we found no significant differences in distributions of open

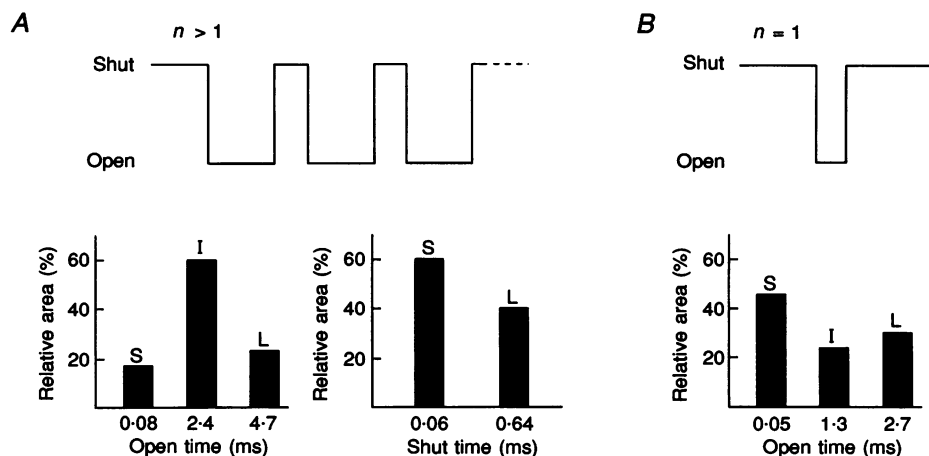


**Figure 8.** Schematic burst structure

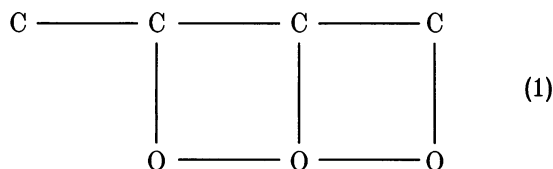
*A*, bursts of more than one opening are represented by an idealized burst (top) containing an unspecified number of open and shut intervals (not drawn to scale). The length of each opening is drawn the same to signify that all the openings during the burst are distributed similarly. Mean values for the open interval distribution time constants and relative areas are shown in the graphs below the traces. The shut intervals during the schematic burst are also drawn the same length because each shut interval was found to have approximately the same distribution. Their distribution is summarized also, with mean values shown. The letters in the graphs indicate the components of short (S), intermediate (I) and long (L) durations. *B*, the openings that were single-opening bursts, in comparison with the openings in lengthier bursts, were more often short duration. Since their distribution did not match those of the other openings, single openings are shown separately. This representation is consistent with findings that the distribution of openings per burst contains two geometric components: one component of unit mean and another with a mean (in our experiments) of approximately two openings per burst (see also Gibb & Colquhoun, 1992). As a result, single-opening bursts arising from both geometries will be found in the interval distributions (Fig. 3A). We can only draw attention to this as, unfortunately, the openings cannot be unambiguously separated from each other because of the overlap between the components.

intervals at any position within bursts of different lengths (see Fig. 3 and text). We also compared distributions of all openings from bursts of two to four openings and again found no dependence on burst length (data not shown). With respect to the shut intervals within bursts, NMDA and GABA<sub>A</sub> receptor bursts are similar: distributions for each of the shut intervals are alike, and do not depend on burst length.

### A model for bursts of more than one opening

Our results have significant mechanistic implications. Mechanisms that have been proposed for other ligand-gated ion channels such as the nicotinic acetylcholine receptor (Dionne, Steinbach & Stevens, 1978; Colquhoun & Hawkes, 1982), Ca<sup>2+</sup>-activated K<sup>+</sup> channel (Magleby & Pallotta, 1983*b*), glutamate receptor (Kerry, Kits, Ramsey, Sansom & Usherwood, 1987) and GABA receptor (Weiss & Magleby, 1989; Twyman *et al.* 1990) appeared at first to be consistent with our results because we found several variations of these mechanisms which described the distributions of all open and shut intervals (see Fig. 1).

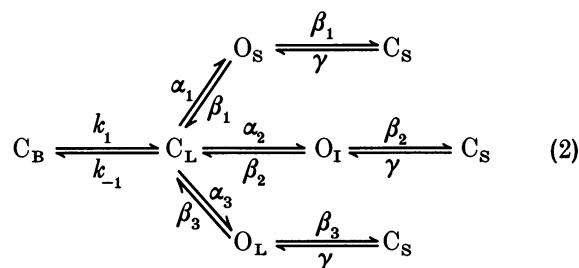
These models have in common a set of connected, closed kinetic states (C) and a set of two or more open states (O) that might be connected to each other. The open and shut states are themselves connected by two or more pathways as required by results from adjacent-states analysis (Blatz & Magleby, 1989) and interval duration autocorrelations (Labarca, Rice, Fredkin & Montal, 1985):



All of these schemes can predict the presence of bursting behaviour. For the nicotinic acetylcholine receptor, Colquhoun & Sakmann (1985) described a version of the above mechanism with two open and three closed states in which the mean open and shut times during bursts are independent of position within the burst. As shown by Colquhoun & Hawkes (1982), however, this type of mechanism can also predict that the openings and gaps during bursts will depend on burst position and length. This happens because the particular state to which the channel opens during a burst will depend upon the closed state to which the previous opening ended. With the addition of two intraburst closed states distal to each open state, a model of this type successfully describes the burst-length dependence of GABA<sub>A</sub> receptor openings (Twyman *et al.* 1990). With respect to our findings from NMDA receptors, however, we could find no variant of the above mechanism that simultaneously predicted the steady-state distributions of open and shut intervals, and openings per burst, while at the same time predicting that each open and shut interval during a burst should be like every other.

Instead, we found that models of the above type that had sufficient complexity to account for the three open and five closed state kinetic components we observed, all predicted significant changes in the open and closed time distributions as a function of position within bursts or burst length. As a result, we chose an alternative type of model to describe our results.

To account for our major result, that each opening and closing during a burst is like every other, we propose a mechanism for burst behaviour in which a single closed state acts as a gateway to the three open states:



The gateway state (C<sub>L</sub>) ensures that each of the three types of opening occur in the same relative proportion to each other regardless of the length of the burst. The gateway also serves as the intraburst long-duration shut state, while the short-duration shut states arise from three closed kinetic states (C<sub>S</sub>) that are distal to the open states. These closed states are assumed to be identical in duration so they contribute only a single (0.06 ms) duration to the distributions of shut times during bursts. In this model, a burst begins when the channel leaves the long-lived C<sub>B</sub> state and begins to undergo transitions between the C<sub>L</sub>, O<sub>S</sub>, O<sub>I</sub>, O<sub>L</sub> and C<sub>S</sub> states. Since C<sub>L</sub> is an intraburst state, a given burst can contain one or all types of opening. The burst ends with a transition back to C<sub>B</sub>. The behaviour of the model is illustrated in Fig. 9, which shows the results of simulations of scheme (2) given the rate constants in Table 2.

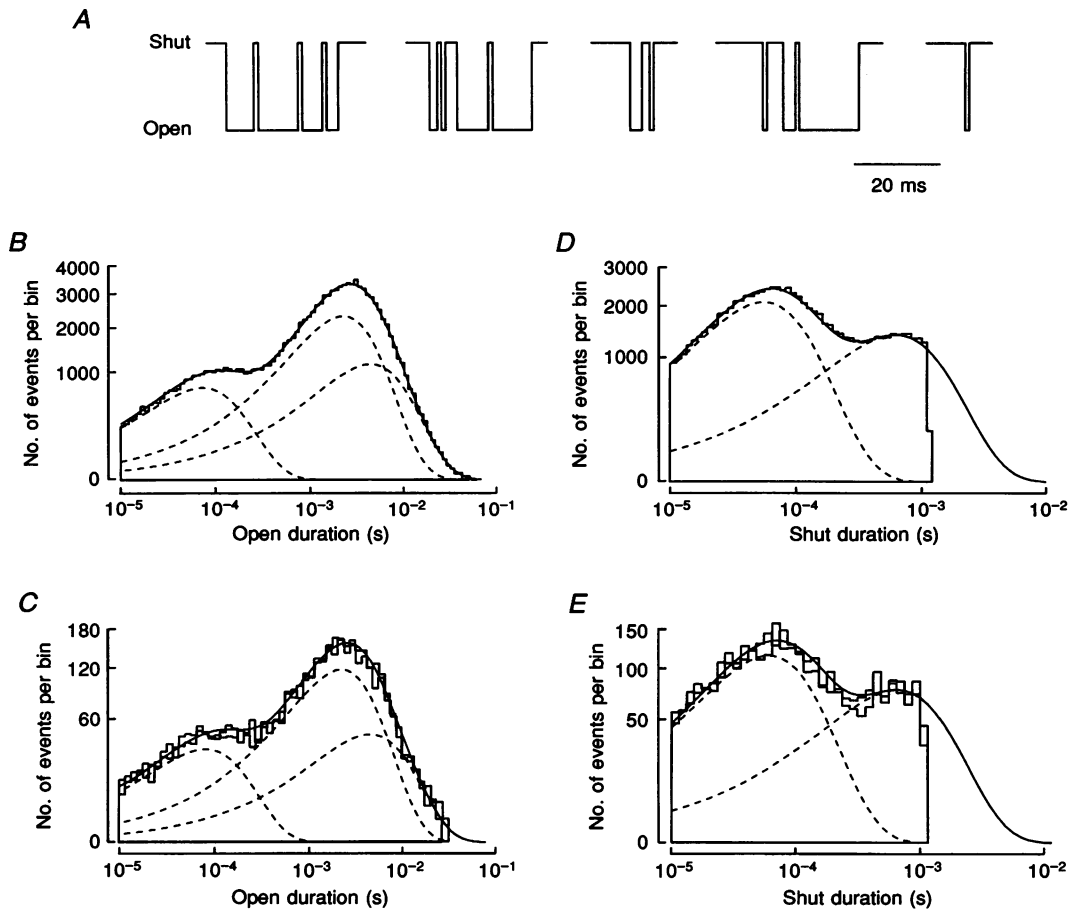
Simulated channel openings (Fig. 9A) illustrate the basic bursting behaviour of the model. As described above for actual currents, the modelled bursts consist of one or more openings, the durations of which range from short to long duration. To analyse this behaviour, simulated channel openings were partitioned into bursts with the same

Table 2. Rate constants for scheme (2) (ms<sup>-1</sup>)

$k_1$	0.10
$k_{-1}$	0.39
$\alpha_1$	0.17
$\alpha_2$	0.60
$\alpha_3$	0.23
$\beta_1$	6.25
$\beta_2$	0.21
$\beta_3$	0.11
$\gamma$	16.67

methods we used for real currents. The histogram of 120 000 simulated open interval durations (Fig. 9B) was fitted with the sum of three exponential components with time constants (and relative areas) of 0.08 ms (0.17), 2.4 ms (0.55) and 4.7 ms (0.27). This distribution is virtually identical to the average distribution obtained from actual

open intervals during bursts (Fig. 8) and to the theoretical distribution calculated from scheme (2) (see legend, Fig. 9C). The open intervals that occurred during bursts had the same distribution. Figure 9C shows a comparison of two distributions, one obtained from the second openings, and the other from the third openings, each from 3586 simulated



**Figure 9. Simulated bursts and interval distributions**

Sequences of simulated open and shut intervals were obtained from scheme (2) by simulation. These intervals were then analysed in an identical manner to that used for the actual intervals. Rate constants (Table 2) were adjusted to yield distributions that were similar to those shown in the summary (Fig. 8). *A*, from the distribution of simulated shut intervals, a critical gap (1.17 ms) was found and used to divide the intervals into bursts. Representative bursts of one or more openings are shown. *B*, the distribution of 120 000 simulated open intervals was fitted with the sum of three exponential components with time constants (and relative areas) of 0.08 ms (0.17), 2.42 ms (0.56) and 4.75 ms (0.27). Compare this distribution to those shown in Fig. 4 and to the distributions from multiple-opening bursts shown in Figs 2 and 3. *C*, duration histograms were constructed for the second and third openings from 3586 simulated bursts that contained only three openings. Both these histograms are shown superimposed with the theoretical distribution calculated from scheme (2): 0.08 ms (0.17), 2.40 ms (0.6) and 4.72 ms (0.23). The histograms in *B* and *C*, and additional simulations (not shown), demonstrated that scheme (2) predicts that each opening in a burst has the same distribution as every other regardless of burst length. *D*, the distribution of 92 866 shut intervals that were contained within 27 057 simulated bursts of all lengths was fitted with two time constants (and relative areas) of 0.06 ms (0.6) and 0.68 ms (0.40). Compare this distribution to those in Figs 5, 6 and 7. *E*, duration histograms were constructed for the first and second shut intervals from 3325 simulated bursts that contained four openings. Each histogram is shown superimposed with the theoretical distribution of 0.06 ms (0.6) and 0.64 ms (0.4). Compare this figure to the histograms in Fig. 6. The histograms in *D* and *E*, and additional simulations (not shown), showed that scheme (2) predicts the same distribution for each shut interval during a burst, regardless of burst length.

bursts of only three openings. Superimposed on both histograms is the theoretical distribution calculated from scheme (2). This and other simulations showed that scheme (2) behaves in a manner consistent with our results: that each opening of a burst had the same distribution regardless of position or burst length.

The fit to the distribution of shut times during bursts obtained by simulation (Fig. 9D) was also in agreement with the data summary (Fig. 8): the fitted time constants (and relative areas) were 0.06 (0.60) and 0.68 ms (0.40). This distribution closely resembles actual distributions for shut intervals during bursts (Figs 5, 6 and 7) because (simulated) shut intervals longer than  $t_c$  (1.17 ms) were excluded. When shut intervals were further sorted with respect to the lengths of bursts or the position during each burst, the distributions of shut intervals were independent of burst length or position, in agreement with our results. This is illustrated in Fig. 9E, in which the distributions of the first and second shut intervals during bursts of four openings each superimpose with the theoretical distribution calculated from scheme (2).

One aspect of the bursting behaviour that was not well captured by the model is the number of openings per burst. The model predicts a single geometric component to this distribution, with a mean of 5.8 openings per burst. In seven patches we measured two components in this distribution, one with a mean (and relative area) of 1.1 openings per burst (0.53) and a second component with a mean of 2.0 openings per burst (0.47). The first component corresponds to the population of single, isolated openings. These openings were short, intermediate, or long duration (Fig. 8B), and their contribution as single-opening bursts caused distributions of first-openings of bursts (Fig. 2B) to be substantially different from the distributions of all the other openings. The reason for this is that the single-opening bursts (which include single-opening clusters) were more often short-duration events than were the openings that occurred during multiple-opening bursts. Hence our cautioning that scheme (2) was designed to describe bursts of two or more openings, although the model correctly predicts that there will also be single-opening bursts whose distributions will be identical to those of the other openings. To account for the separate population of isolated events, scheme (2) would require the addition of one or more very long-lived closed state(s) to which three additional open states had direct access (Colquhoun & Hawkes, 1987; and see Stevens & Lin, 1994). By adding additional states to which the burst can terminate, the number of openings per burst would also be reduced to a value more consistent with observation. These states would also now separate groups of bursts into clusters, and if of sufficiently long duration, would bestow desensitization and inverse autocorrelations upon the mechanism. Such

modifications to the model are beyond the scope of the present work, but are presented in Donnelly & Pallotta (1995). It should also be noted that the rate constants in Table 2 were derived to describe data that were uncorrected for missed events and noise. That being the case, the constants are only approximations to the actual transition rates that would be found if there were no filtering- or noise-induced limitations, and if scheme (2) were indeed correct.

There is another prediction of scheme (2) that could, in principle, be tested. The model predicts that no correlations should be found between the open intervals and their adjacent shut intervals during bursts, since any type of opening can be preceded or followed by any type of shut interval. We tested this prediction by adjacent-states analysis of the actual intervals. In each patch, this relationship (data not shown) showed a clear inverse correlation, such that short-duration open intervals tended to be near to long-duration shut intervals, as previously reported (Gibb & Colquhoun, 1992). However, in six of our seven patches, the slope of this correlation was much less over the range of shut intervals that were less than or equal to the critical gap (i.e. within bursts). In three patches the adjacent-states relationship was flat, while in one patch the slope was positive. While this result supports a mechanism for bursting such as scheme (2), variation in the adjacent-states relationships barred us from any conclusion other than that the model was consistent with these results.

Finally, it must be pointed out that our results were obtained from glutamate receptors activated by NMDA and that our conclusions apply only for that agonist. However, channel kinetics in the presence of the natural neurotransmitter, glutamate, are similar to those obtained with NMDA in that the numbers of components in the distributions of open and shut intervals, and openings per burst, are the same. This suggests that the same numbers of kinetic states participate in the response to either agonist, and that the gating mechanism (whatever it might be) responds similarly to either NMDA or glutamate. An analysis of burst events similar to that presented here, but with glutamate as the agonist, would provide a test of the general applicability of scheme (2). In this regard scheme (2) makes an unyielding prediction: regardless of the actual component weights and means, this gateway type of scheme requires each opening (and closing) to have the same distribution as every other.

### Relationship to macroscopic models

A number of models have been proposed that account for the kinetics of NMDA receptor activation and desensitization. These models were derived from macroscopic currents evoked in neurons or outside-out patches by rapid application of agonists or antagonists (Benveniste, Clements,

- Vyklický & Mayer, 1990; Clements & Westbrook, 1991; Sather, Diéudonné, MacDonald & Ascher, 1992; Clements, Lester, Tong, Jahr & Westbrook, 1992; Lester, Tong & Jahr, 1993). They have in common a single open state and two or more closed states to which the agonists NMDA and glycine bind and initiate channel opening. In most of these schemes, transitions to one or more desensitized states occur directly from a closed-channel state. The conditions of our experiments were quite different: agonist concentrations were fixed and single-channel currents were recorded under steady-state conditions. In fact, the kinetic states that give rise to bursts of openings most probably do not contain any binding steps (Lester *et al.* 1990; Gibb & Colquhoun, 1991; Edmonds & Colquhoun, 1992) and we have modelled them so. Our single-channel model and the macroscopic models can, however, be easily reconciled into a single model that would be consistent with both types of data. Since the open probability during bursts is high (0.9; calculated from data summary in Fig. 8), the burst states in scheme (2) can be substituted for the single open state in the macroscopic models. The resulting mechanism would be consistent with both single-channel and macroscopic-channel behaviour, if the mechanism were modified to allow desensitization to occur primarily from one or more open-channel states (Stevens & Lin, 1994).
- ASCHER, P. & NOWAK, L. (1988). The role of divalent cations in the *N*-methyl-D-aspartate responses of mouse central neurones in culture. *Journal of Physiology* **399**, 247–266.
- BEAL, M. F. (1992). Mechanisms of excitotoxicity in neurologic diseases. *FASEB Journal* **6**, 3338–3344.
- BENVENISTE, M., CLEMENTS, J., VYKLIČKÝ, L. JR & MAYER, M. L. (1990). A kinetic analysis of the modulation of *N*-methyl-D-aspartic acid receptors by glycine in mouse cultured hippocampal neurones. *Journal of Physiology* **428**, 333–357.
- BENVENISTE, M. & MAYER, M. L. (1991). A kinetic analysis of antagonist action at NMDA receptors: evidence for two agonist binding sites. *Biophysical Journal* **59**, 560–573.
- BLATZ, A. L. & MAGLEBY, K. L. (1989). Adjacent interval analysis distinguishes among gating mechanisms for the fast chloride channel from rat skeletal muscle. *Journal of Physiology* **410**, 561–585.
- CLEMENTS, J. D., LESTER, R. A. J., TONG, G., JAHR, C. E. & WESTBROOK, G. L. (1992). The time course of glutamate in the synaptic cleft. *Science* **258**, 1498–1501.
- CLEMENTS, J. D. & WESTBROOK, G. L. (1991). Activation kinetics reveal the number of glutamate and glycine binding sites on the *N*-methyl-D-aspartate receptor. *Neuron* **7**, 605–613.
- COLQUHOUN, D. & HAWKES, A. G. (1981). On the stochastic properties of single ion channels. *Proceedings of the Royal Society B* **211**, 205–235.
- COLQUHOUN, D. & HAWKES, A. G. (1982). On the stochastic properties of bursts of single ion channel openings and of clusters of bursts. *Proceedings of the Royal Society B* **300**, 1–59.
- COLQUHOUN, D. & HAWKES, A. G. (1987). A note on correlations in single ion channel records. *Proceedings of the Royal Society B* **230**, 15–52.
- COLQUHOUN, D. & HAWKES, A. G. (1990). Stochastic properties of ion channel openings and bursts in a membrane patch that contains two channels: evidence concerning the number of channels present when a record containing only single openings is observed. *Proceedings of the Royal Society B* **240**, 453–477.
- COLQUHOUN, D. & SAKMANN, B. (1981). Fluctuations in the microsecond time range of the current through single acetylcholine receptor ion channels. *Nature* **294**, 464–466.
- COLQUHOUN, D. & SAKMANN, B. (1985). Fast events in single-channel currents activated by acetylcholine and its analogues at the frog muscle end-plate. *Journal of Physiology* **369**, 501–557.
- COLQUHOUN, D. & SIGWORTH, F. J. (1983). Fitting and statistical analysis of single-channel records. In *Single-Channel Recording*, ed. SAKMANN, B. & NEHER, E., pp. 191–263. Plenum Press, New York.
- CULL-CANDY, S. G. & USOWICZ, M. M. (1987). Multiple-conductance channels activated by excitatory amino acids in cerebellar neurons. *Nature* **325**, 525–528.
- DIONNE, V. E., STEINBACH, J. H. & STEVENS, C. F. (1978). An analysis of the dose–response relationship at voltage-clamped frog neuromuscular junctions. *Journal of Physiology* **281**, 421–444.
- DONNELLY, J. L. & PALLOTTA, B. S. (1995). Single-channel currents from diethylpyrocarbonate-modified NMDA receptors in cultured rat brain cortical neurons. *Journal of General Physiology* **105**, 837–859.
- EDMONDS, B. & COLQUHOUN, D. (1992). Rapid decay of averaged single-channel NMDA receptor activations recorded at low agonist concentration. *Proceedings of the Royal Society B* **250**, 279–286.
- GIBB, A. J. & COLQUHOUN, D. (1991). Glutamate activation of single NMDA receptor-channel produces a cluster of channel openings. *Proceedings of the Royal Society B* **243**, 39–45.
- GIBB, A. J. & COLQUHOUN, D. (1992). Activation of *N*-methyl-D-aspartate receptors by L-glutamate in cells dissociated from adult rat hippocampus. *Journal of Physiology* **456**, 143–179.
- HOCH, D. B. & DINGLELINE, R. (1986). GABAergic neurons in rat hippocampal culture. *Developmental Brain Research* **25**, 53–64.
- HOLLMANN, M. & HEINEMANN, S. (1994). Cloned glutamate receptors. *Annual Review of Neuroscience* **17**, 31–108.
- HORN, R. (1987). Statistical methods for model discrimination: applications to gating kinetics and permeation of the acetylcholine receptor channel. *Biophysical Journal* **51**, 255–263.
- HOWE, J. R., CULL-CANDY, S. G. & COLQUHOUN, D. (1991). Currents through single glutamate receptor channels in outside-out patches from rat cerebellar granule cells. *Journal of Physiology* **432**, 143–202.
- JAHR, C. E. & STEVENS, C. F. (1987). Glutamate activates multiple single channel conductances in hippocampal neurons. *Nature* **325**, 522–525.
- JAHR, C. E. & STEVENS, C. F. (1990). A quantitative description of NMDA receptor-channel kinetic behavior. *Journal of Neuroscience* **10**, 1830–1837.
- KERRY, C. J., KITS, K. S., RAMSEY, R. L., SANSOM, M. S. & USHERWOOD, P. N. (1987). Single channel kinetics of a glutamate receptor [corrected and republished article originally printed in *Biophysical Journal* (1986) **50**, 367–374]. *Biophysical Journal* **51**, 137–144.

- KORN, S. J. & HORN, R. (1988). Statistical discrimination of fractal and Markov models of single-channel gating. *Biophysical Journal* **54**, 871–877.
- KRISHTAL, O. A. & PIDOPLICHKO, V. I. (1980). A receptor for protons in the nerve cell membrane. *Neuroscience* **5**, 2325–2327.
- LABARCA, P., RICE, J. A., FREDKIN, D. R. & MONTAL, M. (1985). Kinetic analysis of channel gating. Application to the cholinergic receptor channel and the chloride channel from *Torpedo californica*. *Biophysical Journal* **47**, 469–478.
- LESTER, R. A. J., CLEMENTS, J., WESTBROOK, G. L. & JAHR, C. E. (1990). Channel kinetics determine the time course of NMDA receptor-mediated synaptic currents. *Nature* **346**, 565–567.
- LESTER, R. A. J., TONG, G. & JAHR, C. E. (1993). Interactions between the glycine and glutamate binding sites of the NMDA receptor. *Journal of Neuroscience* **13**, 1088–1096.
- MCBAIN, C. L. & MAYER, M. L. (1994). *N*-methyl-D-aspartic acid receptor structure and function. *Physiological Reviews* **74**, 723–760.
- MACDONALD, R. L., ROGERS, C. J. & TWYMAN, R. E. (1989). Kinetic properties of the GABA receptor main conductance state of mouse spinal cord neurones in culture. *Journal of Physiology* **410**, 479–499.
- MCMANUS, O. B. & MAGLEBY, K. L. (1988). Kinetic states and modes of single large-conductance calcium-activated potassium channels in cultured rat skeletal muscle. *Journal of Physiology* **402**, 79–120.
- MAGLEBY, K. L. (1992). Preventing artifacts and reducing errors in single-channel analysis. *Methods in Enzymology* **207**, 763–791.
- MAGLEBY, K. L. & PALLOTTA, B. S. (1983*a*). Burst kinetics of single calcium-activated potassium channels in cultured rat muscle. *Journal of Physiology* **344**, 605–623.
- MAGLEBY, K. L. & PALLOTTA, B. S. (1983*b*). Calcium dependence of open and shut interval distributions from calcium-activated potassium channels in cultured rat muscle. *Journal of Physiology* **344**, 585–604.
- NOWAK, L., BREGESTOVSKI, P., ASCHER, P., HERBET, A. & PROCHIANZ, A. (1984). Magnesium gates glutamate-activated channels in mouse central neurones. *Nature* **307**, 462–465.
- PRESS, W. H., TEUKOLSKY, S. A., VETTERLING, W. T. & FLANNERY, B. P. (1992). Statistical description of data. In *Numerical Recipes in Fortran: The Art of Scientific Computing*, 2nd edn, pp. 603–649. Cambridge University Press, New York.
- SAKMANN, B. & NEHER, E. (1983). *Single-Channel Recording*. Plenum Press, New York.
- SATHER, W., DIEUDONNÉ, S., MACDONALD, J. F. & ASCHER, P. (1992). Activation and desensitization of *N*-methyl-D-aspartate receptors in nucleated outside-out patches from mouse neurones. *Journal of Physiology* **450**, 643–672.
- SIGWORTH, F. J. & SINE, S. M. (1987). Data transformations for improved display and fitting of single-channel dwell time histograms. *Biophysical Journal* **52**, 1047–1054.
- STEVENS, C. F. & LIN, F. (1994). Both open and closed NMDA receptor channels desensitize. *Journal of Neuroscience* **14**, 2153–2160.
- TWYMAN, R. E., ROGERS, C. J. & MACDONALD, R. L. (1990). Intra-burst kinetic properties of the GABA<sub>A</sub> receptor main conductance state of mouse spinal cord neurones in culture. *Journal of Physiology* **423**, 193–220.
- WEISS, D. S. & MAGLEBY, K. L. (1989). Gating scheme for single GABA-activated Cl<sup>-</sup> channels determined from stability plots, dwell-time distributions, and adjacent-interval durations. *Journal of Neuroscience* **9**, 1314–1324.

### Acknowledgements

We thank Dr Karl Magleby for comments on the manuscript. This work was supported by grants NS 29881 (B.S.P.) and NS 08992 (N.W.K.) from the National Institutes of Health.

### Author's present address

N. W. Kleckner: Department of Biology, Bates College, Lewiston, ME 04240, USA.

Received 31 August 1994; accepted 10 January 1995.